

E-ISSN: 2229-7677 • Website: <a href="www.ijsat.org">www.ijsat.org</a> • Email: editor@ijsat.org

# Molecular Docking method and spectral analysis with calculations on N-Phenylanthraniliacid

# M. Govindarajan<sup>1,2</sup>

<sup>1</sup>Department of Physics, Avvaiyar Government College for Women (AGCW), Karaikal, Puducherry 609 602, India

<sup>2</sup>Arignar Anna Government Arts and Science College for Women (AAGASC), Karaikal Puducherry 609602, India

#### **Abstract**

In this work, the collective analyses of experimental and simulated fixed out by Infrared spectroscopy for N-Phenylanthraniliacid (C13H11N1O2) (N-PHARA) molecule in solid phase recorded. It will meet optimized geometries, which correspond to true energy minima, as revealed by the lack of imaginary frequencies in the vibrational mode calculation. Vibrational analysis at B3LYP/6-311++G(d,p) leve. The calculated HOMO and LUMO values for the molecules are also given with number of states 10. The electronic and excited state properties have been determined by TD-DFT method. The results of the calculations were applied to simulated spectra of the N-PHARA compound, which show good arrangements with observed spectra. The scaled B3LYP/6-311++G(d,p) results show the best results with the experimental values over the other methods. The aim of RDG analysis is to look into non-covalent interactions in molecular and bring out their presence both internally and externally. In addition, molecular electrostatic potential (MEP) and electron density (ED) map of the N-PHARA were performed.

**Keywords**: FT-IR; FT-RAMAN; HOMO-LUMO; DFT/B3LYP and HF.

# 1. Introduction INTRODUCTION

The N-phenylanthranilic acid is used as an intermediate in the synthetic thinking of pharmaceutically important molecules such as anti-malarials, anti-inflammatory and anti-neoplatics. Benzoic acid is also found in animals. Its derivatives are the constituent parts of many enzymes and other biologically important molecules. It also occurs widely in plants and animals tissues along with Vitamin-B complex and is used in miticides, contrast media in urology, cholocystrographic examinations and in the manufacture of pharmaceuticals. The compound N-phenylanthranilic acid is used as a common intermediate in the synthesis of pharmaceutically important molecules such as anti-malarials, anti-inflammatory and anti-neoplatics. The derivatives of benzoic acid are known to enhance the action of local anaesthetics, as evaluated by measuring the pain sensibility of human skin and the action potentials from the crayfish giant axon and the rat cervical vagus in vitro. Benzoic acid derivatives, such as bromo/chloro benzoic acid and amino benzoic acid [Anthranilic acid], have active bacteriostatic and



E-ISSN: 2229-7677 • Website: <a href="www.ijsat.org">www.ijsat.org</a> • Email: editor@ijsat.org

fragrant properties, hence they are used in pharmaceutical and perfumery industry[2-4]. The harmonic vibrational frequencies were calculated and the scaled values have been compared with experimental spectra. Hence a lot works have been reported in the literature [5–16] from time to time on these molecules..However, no vibrational study based on DFT has been reported either on anthranilic acid or on bromo benzoic acids, in particular the comparative vibrational analysis of these molecules.

#### 2. Experimental procedure

The molecule below investigating namely N-PHARA bought from Sigma-Aldrich chemicals, U.S.A with spectroscopic level and it was used as such without any further purification. The FT-IR spectrum of the compound has been recorded in Perkin-Elmer 180 Spectrometer in the range of 4000–400 cm $^{-1}$ . The spectral resolution is  $\pm$  2 cm $^{-1}$ . The FT-Raman spectrum of the compound was also recorded in the same instrument with FRA 106 Raman module equipped with Nd: YAG laser source operating in the region 100-4000 cm $^{-1}$  at 1.064 µmline widths with 200 mW powers. The spectra were recorded scanning speed of 30 cm $^{-1}$  min $^{-1}$  and spectral width 2cm $^{-1}$ . The frequencies of all sharp bands are accurate to  $\pm$  1 cm $^{-1}$ .

#### 3. Quantum chemical calculations

The calculations have been performed DFT (B3LYP) method with 6-311++G(d,p) basis set using Gaussian 09 program [17]. The wavenumbers calculated at the range of wave numbers above 1700 cm<sup>-1</sup> are scaled as 0.958 and below 1700 cm<sup>-1</sup> scaled as 0.983 for B3LYP/6-311++G(d,p) [18]. The appointments of the calculated normal modes have been made on the basis of the corresponding PEDs. The PEDs are calculated from quantum chemically computed wavenumbers using VEDA program [19]. Gauss view program [20] has been considered to get visual animation and also for the verification of the normal modes assignment. The electronic absorption spectra for optimized N-PHARA calculated with time dependent density functional theory (TD-DFT) at B3LYP/6-311++G (d,p) level.

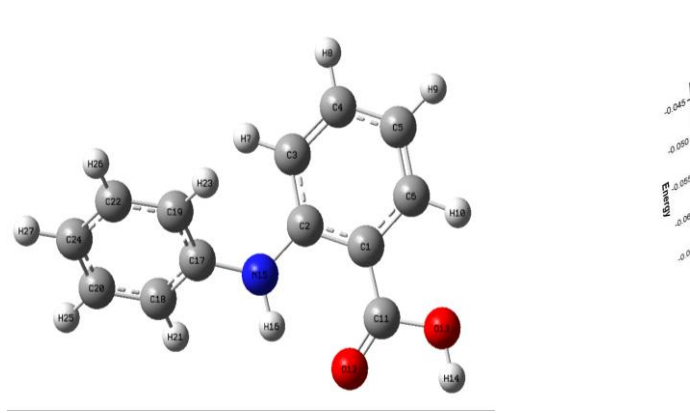
#### 4. Results and discussion

#### 4.1 Geometry analysis

The N-PHARA have two substituent group attached to form the molecule. The optimized DFT geometries by B3LYP/6-311++G(d,p) and molecular structure of the N-PHARA with atom numbering are shown in Fig.1. The internal coordinates describe the position of the atoms in terms of distances, angles and dihedral angles with respect to an origin atom. By allowing the relaxation of all parameters, the calculations are made up of scan coordinate1 C2-N15-C17-C19 and scan coordinate2 C3-C2-N15-C17 by rotating angle 0 to 360. It will meet optimized geometries, which correspond to true energy minima, as revealed by the lack of imaginary frequencies in the vibrational mode calculation. The symmetry coordinates are constructed using the set of internal coordinates. In this study, the full sets of 121 standard internal coordinates for N-PHARA are presented in Fig.2. This structure was found to be global minimum energy with value E=-0.06811 eV.



E-ISSN: 2229-7677 • Website: www.ijsat.org • Email: editor@ijsat.org



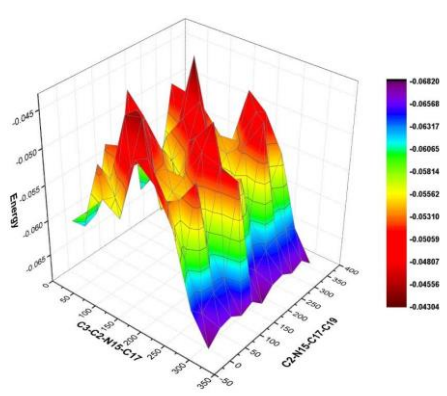


Fig.1 Fig.2

#### 4.2 Ultraviolet spectra analysis

The highest occupied molecular orbitals (HOMOs) and the lowest-lying unoccupied molecular orbitals (LUMOs) are named as frontier molecular orbitals (FMOs). The FMOs play a major role in the optical and electrical properties, as well as in UV–Vis spectra [21]. Gauss-Sum 2.2 Program [22] was used to calculate group contributions to the molecular orbital (HOMO and LUMO) as shown in Fig. 3. The HOMO is the power to give an electron, LUMO as represents

the ability to obtain an electron. The gap between HOMO and LUMO energy determines the kinetic stability, chemical responsiveness and, optical polarization and chemical hardness-softness of a N-PHARA.

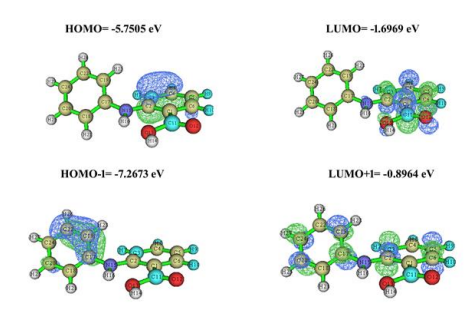


Fig.3

Table 1. Theoretical electronic absorption spectra of 4-chlorophenyl-4-chlorobenzenesulfonate, (absorption wavelength  $\lambda$  (nm), excitation energies E (eV) and oscillator strengths (f)) using TD-DFT/B3LYP/6-311++G(d,p) method in gas and solvent ( Gas and DMSO ) phase.

Solvents	λ (nm)	E (eV)	(f)	Major contribution
Gas	237.9	5.2070	0.053	H-2->LUMO (53%)
	225.5	5.4925	0.026	H-4->LUMO (43%)
	223.8	5.5333	0.039	H-3->LUMO (49%)



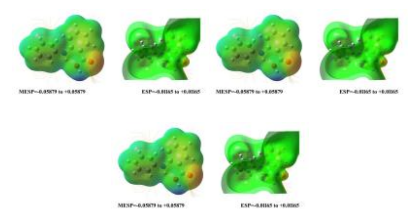
E-ISSN: 2229-7677 • Website: www.ijsat.org • Email: editor@ijsat.org

	213.4	5.8053	0.022	HOMO->L+2 (42%)
	211.7	5.8499	0.021	HOMO->L+2 (33%)
	183.3	6.7411	0.836	H-2->L+1 (53%)
	179.7	6.8898	0.264	HOMO->LUMO (51%)
	174.8	7.0761	0.406	H-3->L+1 (41%)
	170.0	7.2690	0.696	H-2->L+1 (34%)
	165.4	7.4676	0.683	HOMO->L+2 (36%)
	238.1	5.2110	0.056	H-2->LUMO (53%)
	225.7	5.4958	0.027	H-4->LUMO (42%)
	224.0	5.5383	0.042	H-3->LUMO (50%)
	213.5	5.8083	0.024	HOMO->L+2 (37%)
DMSO	211.9	5.8562	0.022	HOMO->L+2 (37%)
	183.9	6.7638	0.889	H-2->L+1 (31%)
	179.9	6.8983	0.259	HOMO->LUMO (51%)
	175.2	7.0909	0.401	H-3->L+1 (41%)
	170.5	7.2929	0.737	H-2->L+1 (38%)
	166.0	7.4926	0.688	HOMO->L+2 (36%)

In order to measure the energetic behavior of a N-PHARA compound, we carried out calculations in Gas and DMSO with number of states 10. The calculated energy values of HOMO and HOMO-1 are -5.7505 and -7.2673 eV Gas, respectively. LUMO and LUMO+1 is -1.6969 and -0.8964 eV in the same respectively. The value of energy gap between the HOMO and LUMO is -7.4465 eV in Gas, respectively.

The calculated HOMO and LUMO moment values for the molecules are also given for Gas DMSO in the Table 2. An ultraviolet spectra analysis of N-PHARA has been investigated in Gas and DMSO by theoretical calculation. On the basis of fully optimized ground-state structure, TD-DFT/B3LYP/6-311++G(d, p) calculations were fixed it to determine the low-lying excited states of N-PHARA The calculated absorption maxima values have been found to be as for gas at DFT/B3LYP/6-311++G(d,p) method. It is seen from Table 2, calculations performed at gas are close to each other when compared with other phases.

#### 4.3 Molecular and electrostatic potential



In the present study, a 3D plot of molecular electrostatic potential (MEP) and electron density (ED) map of N-PHARA I fixed it in Fig. 4. In the majority of the MEPs, while the maximum negative region, which preferred site for electrophilic attack indications as red colour, the maximum positive region which preferred site for nucleophilic attack symptoms as blue colour. The importance of MEP lies in the



E-ISSN: 2229-7677 • Website: <a href="www.ijsat.org">www.ijsat.org</a> • Email: editor@ijsat.org

fact that it collectedly exhibits molecular shape as well as positive, negative and neutral electrostatic potential regions in terms of colour grading (Fig. 4) and is very useful in research of molecular structure with its physiochemical property relationship [23-25].I fixed it different values of the electrostatic potential at the surface are represented by different colors. Potential increases in the order red < orange < yellow < green < blue. The color code of this map is in the range of -0.05879 a.u. (deepest red) to 0.05879 a.u. in compound. Where blue indicates the strongest attraction and red indicates the strongest repulsion. The ED value of the N-PHARA is found to be within the range -0.01165 to +0.01165 a.u. The regions having the positive potential are over all hydrogen atoms. I fixed it front and side view of carbon in N-PHARA is having green colour, and it shows neutral potential. According to these calculated results, the MEP map shows that the negative potential sites are on rbon and chlorine atoms as well as the positive potential sites are around hydrogen atoms.

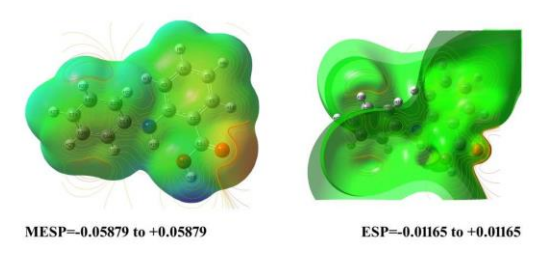


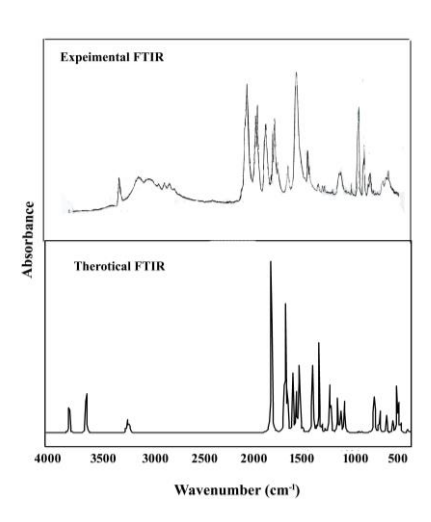
Fig 4

#### 4.4 Mode analysis

The maximum number of potentially observable fundamentals of a non-linear molecule, which contains N atoms is equal to (3N-6), apart from three translational and three rotational degrees of freedom [26, 27]. Hence, N-PHARA molecule, that was planar, has 27 atoms with 75 normal modes of vibrations and considered under  $C_s$  point group symmetry. The fundamental modes are distributed in the  $C_s$  symmetry species as:  $\Box_{vib} = 51A' + 24A''$ . Here, A' is symmetric planer and A'' asymmetric non-planer vibrations. All vibrations are active both in Raman and infrared absorption. The detailed vibrational assignments of the experimental wavenumbers are I fixed it normal mode analyses, and a comparison with theoretically scaled wavenumbers with PED by B3LYP methods. Since the scaled wavenumbers following B3LYP/6-311++G(d,p) method are fixed it closest to experimental data than the results obtained using other methods. The observed and simulated FT-IR and FTRaman spectra of N-PHARA are shown in Fig. 5 and 6, respectively. The observed and scaled theoretical frequencies using DFT/B3LYP/6-311++G(d,p) basis set with PEDs are fixed it in the Table 3.



E-ISSN: 2229-7677 • Website: <a href="www.ijsat.org">www.ijsat.org</a> • Email: editor@ijsat.org



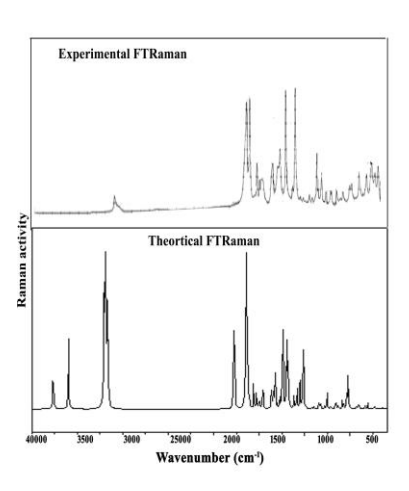


Fig .5 Fig .6



E-ISSN: 2229-7677 • Website: www.ijsat.org • Email: editor@ijsat.org

Table 2: Experimental (FT-IR) wavenumbers and detailed assignments of theoretical wavenumbers of along with potential energy distribution

		Experimenta	Experimental Experimental		Theoretical	
Sl.No	Sy			B3LYP	B3LYP	
		FTIR	FTRaman	Unscaled	scaled	With PED
1.	A"			34	34	φCCC(34)
2.	A"			40	39	φCCC(33)
3.	A"			61	60	φCCC(32)
4.	A"			82	81	φCCC(36)
5.	A"		140 vw	141	139	φCCC(32)
6.	A"		192 vw	195	191	φCCC(39)
7.	A"			233	229	φCCC(32)
8.	A"		240 vw	243	238	φCCC(39)
9.	A"			311	306	φCCC(36)
10.	A"		340 vw	345	339	φCO(32)
11.	A"			404	397	φCO(38)
12.	A"			418	411	φCN(39)
13.	A"		430 vw	433	426	φCN(35)
14.	A'	490 vw		499	491	βCCC(51)
15.	A'			517	509	βCCC(42)
16.	A'	510 vw		521	512	βCCC(45)
17.	A'		530 w	535	526	βCCC(49)
18.	A'	560 vw		574	564	βCCC(49)
19.	A'		590 vw	593	583	βCCC(44)
20.	A'			632	621	βCCC(48)
21.	A'	630 vw		639	628	βCCC(50)
22.	A'		650 vw	659	648	βCCC(52)
23.	A'	695 vs		705	693	βCO(49)
24.	A'		710 vw	717	705	βCO(50)
25.	A'			752	739	βCN(52)
26.	A'	750 vs		763	750	βCN(53)
27.	A"		765 w	778	765	φNH(52)
28.	A"			804	790	φOH(55)
29.	A"		810 vw	831	817	φCH(59)
30.	A"		830 m	845	831	φCH(59)
31.	A"		865 vw	878	863	φCH(55)
32.	A"	885 vw		903	887	φCH(55)
33.	A"	900 vw		918	903	φCH(58)
34.	A"	965 vw		980	963	φCH(61)
35.	A"		970 vw	988	971	φCH(59)
36.	A"			997	980	φCH(62)
37.	A"			1002	985	φCH(58)
38.	A'		1000 vw	1014	997	γCC(61)
39.	A'	1030 vw		1048	1030	γCC(65)
40.	A'	1035 vw		1053	1035	γCC(63)
41.	A'		1065 vs	1089	1070	γCC(72)



E-ISSN: 2229-7677 • Website: <a href="www.ijsat.org">www.ijsat.org</a> • Email: editor@ijsat.org

42.	A'		1090 vw	1104	1086	γCC(69)
43.	A'		1070 111	1122	1102	γCC(62)
44.	A'	1160 m		1181	1161	γCC(65)
45.	A'	1100 III		1187	1167	γCC(62)
46.	A'		1175 vs	1199	1179	γCC(64)
47.	A'		1175 VS	1220	1199	γCC(65)
48.	A'		1225 vw	1242	1221	γCC(66)
49.	A'	1250 vs	1223 VW	1274	1252	γCC(72)
50.	A'	1230 VS		1303	1281	γCO(70)
51.	A'		1310 vw	1329	1306	γCO(72)
52.	A'		1310 VW	1347	1324	γCN(69)
53.	A'	1335 m		1354	1331	γCN(65)
54.	A'	1333 III		1370	1347	βCH(78)
55.	A'	1440 vs		1461	1436	βCH(76)
56.	A'	1440 VS	1460 vw	1491	1466	βCH(66)
57.	A'	1475 vs	1400 vw	1500	1474	βCH(75)
58.	A'	1505 vs		1500	1501	βCH(78)
	A'	1303 VS		1559		. ` ` ′
59.		1500			1533	βCH(66)
60.	A'	1580 vs	1605	1613	1585	βCH(72)
61.	A'		1605 vs	1633	1606	βCH(75)
62.	A'	1.120	1610 s	1641	1614	βCH(82)
63.	A'	1630 vs		1649	1621	βNH(72)
64.	A'			1773	1698	βΟΗ(65)
65.	A'	3030 vw		3162	3029	γCH(99)
66.	A'			3168	3035	γCH(98)
67.	A'			3169	3036	γCH(99)
68.	A'			3178	3045	γCH(97)
69.	A'			3190	3056	γCH(98)
70.	A'			3191	3057	γCH(99)
71.	A'	3060 vw		3197	3063	γCH(98)
72.	A'	3070 vw		3205	3071	γCH(100)
73.	A'		3080 vw	3210	3075	γCH(98)
74.	A'	3440 w		3596	3445	γNH(99)
75.	A'			3764	3606	γOH(98)

#### 4.1.1 C-H vibrations

The aromatic derivatives are giving rise to C-H stretching, C-H in-plane and C-H out-of-plane bending vibrations. Aromatic compounds commonly exhibit multiple weak bands in the region 3100–3000 cm<sup>-1</sup> [28] due to aromatic C-H stretching vibrations. In pure naphthalene I fixed it in the region 3080–3000 cm<sup>-1</sup>. They are not appreciably affected by the nature of the substituent [29-31]. All the C-H stretching vibrations are very weak in intensity in the N-PHARA. Here, the C-H vibrations of the title compound are observed at 3030-3070 cm<sup>-1</sup> in FT-IR spectrum with very weak intensities. This mode I fixed it in the range 3029-3075 cm<sup>-1</sup> with B3LYP/6-311++G(d,p).

The bands due to C-H in-plane bending vibrations I fixed it in the region 1000–1300 cm<sup>-1</sup> [32]. For this compound, the C-H in-plane bending vibrations were observed at four vibrations in FT-IR and three in



E-ISSN: 2229-7677 • Website: www.ijsat.org • Email: editor@ijsat.org

FTRaman. The theoretically scaled vibrations by B3LYP/6-311++G (d,p) level method also shows good agreement with experimentally recorded data.

The C-H out-of-plane bending vibrations I fixed it in the region 980-717 cm<sup>-1</sup> in [32]. The vibrations are identified at three in FT-IR and four in FTRaman are assigned to C-H out-of-plane bending for N-PHARA. All vibrations I fixed it as pure mode except first one from PED values. The C-H out-of-plane bending vibrations are also lie in the characteristic region

#### 4.1.2 Ring vibrations

The aromatic ring modes I fixed it more C-C bands. The ring stretching vibrations are in the region 1300-1000 cm<sup>-1</sup> [33, 34]. Most of the ring modes I fixed it by the substitution of aromatic ring. In present study, the bands with are of different intensities in region 1000-1250 cm<sup>-1</sup> in FT-IR and FTRaman have been assigned to C-C stretching vibrations. The theoretically calculated values at 997-1252 cm<sup>-1</sup> by B3LYP/6-311++G(d,p) method. It shows the theoretic values excellent agreement with experimental data. All these vibrations are fixed modes in PED except their and evident by its few strong intensities. As expected, the in-plane deformations and higher frequencies than the out-of-plane vibrations.

#### 4.1.3 O-H and N-H vibrations

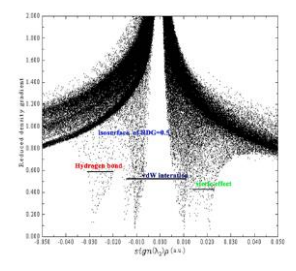
The mixing of vibrations is possible due to the lowering of molecular symmetry and the presence of heavy atoms [35-36]. According to these early reports, the N-H stretching band I fixed it around 505–380 cm $^{-1}$ . In FT-IR spectrum of N-PHARA, a very weak band at 3440 cm $^{-1}$  is assigned to N-H stretch vibration. The theoretical wavenumber of N-H stretching vibration 3445 cm $^{-1}$  by B3LYP/6-311++G(d,p) nearly merge well with the experimental value. The N-H-Cl in-plane bending and out-of-plane bending vibrations are expected to the bands, respectively. The stretch vibration for O-H vibrations is not able match the value. The computed values for O-H in-plane and out-of-plane bending vibrations by B3LYP/6-311++G(d,p) method nearly coincides with experimental values.

#### 4.2 Analysis of molecule Reduced density gradient (RDG)

The aim of RDG analysis is to look into out their presence both internally and externally. The Fig.7 shows the RDG plot of the molecule in question. The RDG grid is drawn between RDG and  $[(\lambda_2) \ \rho]$  a.u. Here, the symbol  $(\lambda_2) \ \rho$  is the second eigenvalue of the electron density. In the figure, the value of the symbol  $(\lambda_2) \ \rho > 0$  represents by the value -0.015 to -0.05 as negative interaction, while the value of the symbol  $(\lambda_2) \ \rho < 0$  represents by the value +0.015 to +0.050 as positive interaction. The symbol  $(\lambda_2) \ \rho = 0$  is the weak van der Waals interaction and  $\lambda_2$  has a range from -0.050 to 0.010. RDG plot shows a positive peak identifying insufficiency in the benzene ring [37]. The positive peaks are between spikes in the picture represent the attraction of hydrogen atoms. The native peak represents repulsion hydrogen atoms. The Vander waa',s interaction is from -0.05 to +0.10. Thus, RDG elements confirm the interaction site in the molecular structure of the compound.



E-ISSN: 2229-7677 • Website: <a href="www.ijsat.org">www.ijsat.org</a> • Email: editor@ijsat.org



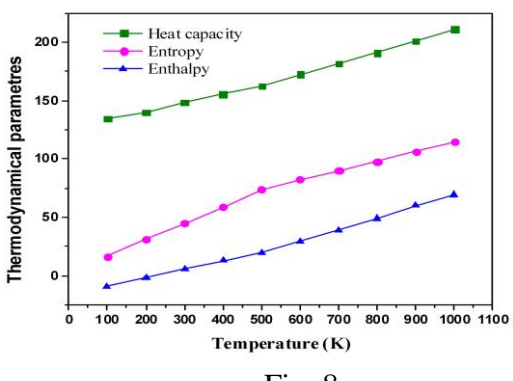


Fig.7

Fig.8

#### 5. Conclusion

The infrared vibration I fixed it and assigned to N-PHARA molecular crystal. The normal co-ordinate of molecule I fixed it DFT-B3LYP method with 6-311++G (d, p) basis set and HF method with 6-311++G(d, p) basis sets. The estimated bond angle values suggest that the ring of the molecule I fixed it due to the steric and electronic effects. The correlation equations between heat capacities, entropies, enthalpy changes and temperatures are fixed it by quadratic polynomial formulas. The energy break of HOMO-LUMO explains the charge shift interaction in an N-PHARA, which influences the physiologic and biological activity of the molecule. The HOMO-LUMO passage involves an electron density transfer from chlorine atom. The calculations are executed when Gas and DMSO are near to each other. The maps are in the range between -0.05879 a.u. (deepest red) to 0.05879 a.u. in N-PHARA. The mean difference between experimental and calculated (B3LYP/6-311++G(d,p)) values of vibrations is only 3 cm<sup>-1</sup>. The C-H vibrations of the title molecule are observed in FT-IR spectrum with very weak intensities. The calculated frequencies by B3LYP/6-311++G(d,p) I fixed it with experimental wavenumbers. The RDG elements confirm the interaction site in the molecular structure of the compound. The symbol is the weak van der Waals interaction and  $\lambda 2$  has a range from -0.050 to 0.010. The thermodynamic properties entropy, enthalpy and heat capacity are from 0 to 1000 K and the curve for each also can be determined.

#### References

- 1. http://en.wikipedia.org/wiki/Benzio\_acid.
- 2. Masui, Coord. Chem. Rev. 957 (2001) 219.
- 3. M. Pagannone, B. Formari, G. Matt G el, Spectrochim Acta A Molecular spectroscopy, 43, (1987) 621
- 4. N.Sundaraganesan, B.Anand, B.Dominic Joshua, Spectrochim Acta A;65 (2006) 1053–62
- 5. K.Yesook, Katsunosuke Machida, Spectrochim Acta A Molecular spectroscopy, 42, (1986) 881
- 6. I. Chalakkal Jose, A Anagha, Belhkhar and S.Mangala Agashe, Spectrochim Acta A Molecular spectroscopy, 44, (1988) 899
- 7. S. Shaik, A. Skurki, D. Danovich, P.C. Hiberty, Chem. Rev. 101 (2001) 1501.
- 8. M.Karabacak, M.Kurt, Spectrochim Acta A 71(2008) 876–83
- 9. Y. Akkaya, S.Akyuz, Vibrational Spectroscopy 42 (2006) 292–301.



E-ISSN: 2229-7677 • Website: <a href="www.ijsat.org">www.ijsat.org</a> • Email: editor@ijsat.org

- 10. C.S.Jean, S.Costa, S.Denise. Cordeiro, C.Antonio. Sant'Ana, Liane M.Rossi, S.Paulo, Santos, Paola Corio, Vibrational Spectroscopy 54 (2010) 133–136
- 11. Y.Ye, M. Ruan, Y.Song, YY.Li, W.Xie, Spectrochim Acta A 68(2007) 85–93
- 12. G.Rauhut, P. Pulay, J. Phys. Chem. 99 (1995) 3093–3100.
- 13. S. Mohan, D. Arul Dhass, Ind. J. Phys. 67B (1993) 403.
- 14. Y. Sarrafi, M. Mohadeszadeh, K. Alimohammadi, Chin. Chem. Lett. 20 (2009) 784.
- 15. Mehmet Karabacak, Dilek Karagoz, Mustafa Kurt, Spectrochim. Acta 72A (2009) 1076–1083
- 16. W. Zhang, G. Pugh, Tetrahedron 59 (2003) 3009
- 17. M.J. Frisch et al, Gaussion 09 Program, Gaussian, Inc., Wallingford, CT, 2004.
- 18. M.Karabacak, A.Coruh, M. Kurt, J. Mol.Struct. 892 (2008) 125-131.
- 19. M.H. Jamróz, Vibrational Energy Distribution Analysis, VEDA 4, Warsaw, 2004.
- 20. A. Frisch, A.B. Nielsen, A.J. Holder, Gaussview Users Manual, Gaussian Inc., Pittsburg.
- 21. R.Zhang, B.Dub, G.Sun, Y.Sun, Spectrochim. Acta A 75 (2010) 1115–1124.
- 22. I.Fleming, Frontier Orbitals and Organic Chemical Reactions, Wiley, London, 1976.
- 23. J.S. Murray, K. Sen, Molecular Electrostatic Potentials, Concepts and 399 Applications, Elsevier, Amsterdam, 1996.
- 24. E.Scrocco, J.Tomasi, in: P.Lowdin (Ed.), Advances in Quantum Chemistry, Academic Press, New York, 1978.
- 25. J. Sponer, P. Hobza, Int. J. Quant. Chem. 57 (1996) 959.
- 26. R.M.Silverstein, G.C.Bassler and T.C.Morrill, Spectrometric identification of organic compounds, John Wiley, Chichester, 1991.
- 27. G.Socrates, Infrared and Raman Characteristic Group Frequencies—Tables and Charts.third ed., Wiley, New York, 2001.
- 28. V.Krishnakumar, R.J.Xavier, Indian J.Pure Appl. Phys., 41 (2003) 597.
- 29. N.B.Colthup, L.H. Daly, S.E. Wiberley, Introduction to Infrared and Raman Spectroscopy, Academic Press, New York, 1990.
- 30. F.R. Dollish, W.G. Fateley, F.F. Bentley, Characteristic Raman Frequencies of Organic Compounds, Wiley, New York, 1997.
- 31. G. Varsanyi, Vibrational Spectra of Benzene Derivatives, Academic Press, New York, 1969.
- 32. A. Srivastava, V.B. Singh, Indian J. Pure. Appl. Phys 45 (2007) 714-720.
- 33. D.Lin–Vien, N.B.Colthup, W.G.Fateley, J.G Grasselli, The Handbook of Infrared Raman Characteristic Frequencies of Organic Molecules, Academic Press, Boston, MA, 1991.
- 34. C.Surisseau, P.Marvell, J.Raman Spectro. 25(1994) 447
- 35. K.C.Medhi, R.Barman, M.K.Sharma. Indian. J. Phys 68B (1994) 189.
- 36. P.S. Peek, D.P.Mcdermoot, Spectrochim. Acta 44 (1988) 371-377.
- 37. R S, Mahalakshmi S, Vetrivelan V, Irfan A, Muthu S, Heliyon., 2023 May 13;9(5):e16066.